BUILDING A PREDICTIVE MODEL OF SUBMERGED AQUATIC VEGETATION FOR ATLANTIC BRANT USING REMOTE SENSING AND IN-SITU SAMPLING

by

Harry Colmorgen

A thesis submitted to the Faculty of the University of Delaware in partial fulfillment of the requirements for the Master of Science in Wildlife Ecology.

Summer 2020

© 2020 Harry Colmorgen
All Rights Reserved

BUILDING A PREDICTIVE MODEL OF SUBMERGED AQUATIC VEGETATION FOR ATLANTIC BRANT USING REMOTE SENSING AND IN-SITU SAMPLING

by

Harry Colmorgen

Approved: _____
Christopher K. Williams, Ph.D.
Professor in charge of thesis on behalf of the Advisory Committee

Approved: _____
Jacob L. Bowman, Ph.D.
Chair of the Department of Entomology and Wildlife Ecology

Approved: _____
Mark Rieger, Ph.D.
Dean of the College of Agriculture and Natural Resources

Approved: _____
Douglas J. Doren, Ph.D.
Interim Vice Provost for Graduate and Professional Education and
Dean of the Graduate College

ACKNOWLEDGMENTS

I would like to thank and acknowledge Dr. Chris Williams for giving me the opportunity to pursue this research endeavor. Without his assistance and knowledge of Atlantic brant, this project would not have been possible. I would also like to thank my committee members, Dr. Kyle McCarthy and Dr. Michael O'Neal, who have provided an abundance of knowledge and assistance to my project. A special thank you to the United States Fish and Wildlife Service for providing necessary financial assistance to fund this project. Furthermore, thank you to Forsythe National Wildlife Refuge and Wertheim National Wildlife Refuge, who provided housing and assistance when traveling to my different study areas. Thank you to Paul Castelli and Ted Nichols who offered their knowledge and years of experience with Atlantic brant in New Jersey.

I would like to thank all the University of Delaware Field Ecology Lab technicians, even those that did not contribute directly to my work, as they provided moral support and assisted as much as possible, when needed. Thank you to my dedicated lab technicians, Emily Slingerland, Kelly Holland, Dominique Lester, and Caylen Wolfer, who endured long hours of sorting vegetation samples. Special thank you to my field technicians, Tom Baxter and Cody Meyer, who were tasked with working in adverse conditions during the winter to collect all vegetation samples by boat in Long Island, New York and New Jersey. Their knowledge of navigating the intercoastal waterways was pivotal in staying safe in trying weather. I would also like to thank my fellow graduate students, Clark Nissely and Phil Coppola, who provided

knowledge and assistance in planning field work, offered insight on statistical analysis, and provided comic relief.

Lastly, I would like to give a tremendous thank you to my friends and family for their encouragement and support to complete this part of my life. Thank you to my parents for helping me reach this point in my education and always supporting all my endeavors. The greatest support and biggest thank you is to my wife, Sara, who has provided unrelenting support on this long journey and stuck by me through the many hours of lab work, field work, and late nights working on my thesis. Thank you for hanging in there through it all.

TABLE OF CONTENTS

LIST OF TABLES vi
LIST OF FIGURES vii
ABSTRACT ix

Chapter

1 BUILDING A MODEL OF SUBMERGED AQUATIC VEGETATION FOR ATLANTIC BRANT 1

Introduction 1
Study Area 7
Methods 9

Initial mapping of potential submerged aquatic vegetation 9
Field Collection of SAV and Environmental Covariates: 10
Laboratory Analysis 12
Analysis and modeling 13

Results 18
Discussion 33
REFERENCES 41

LIST OF TABLES

Table 1: The sampling errors that occurred when conducting field collection of SAV. 22

Table 2: Of the total number of sites that NDVI predicted SAV (eelgrass, *Ulva/Enteromorpha*, and Rhodophyta) present (New Jersey [N=107] and Long Island, New York [N=67], the number and percent accuracy of study sites that SAV was physically observed. This includes the null samples that included SAV. 23

Table 3: Twenty-two a priori models (AICc, ΔAIC, and AIC weight ω values) predicting the presence of *Ulva* and *Enteromorpha* from 6 site level environmental variables in intertidal New Jersey and Long Island, New York, 2015–2016. 24

Table 4: Twenty-two a priori models (AICc, ΔAIC, and AIC weight ω values) predicting the presence of eelgrass from 6 site level environmental variables in intertidal New Jersey and Long Island, New York, 2015–2016. 25

Table 5: Twenty-two a priori models (AICc, ΔAIC, and AIC weight ω values) predicting the presence of Rhodophyta algae from 6 site level environmental variables in intertidal New Jersey and Long Island, New York, 2015–2016. 26

Table 6: The calculated thresholds determined in R compared to an arbitrary threshold of 0.5. 27

Table 7: The estimated carrying capacity for *Ulva/Enteromorpha*, Rhodophyta, and eelgrass assumptions of a complete pull of eelgrass and an assumption that clipping of eelgrass occurs in centimeter increments after their 40 cm reaching capability for Long Island, New York and coastal New Jersey, USA during winter 2015-2016. The estimated carrying capacity for both algae types assuming they are not depth limited due to the ability to be free floating and not permanently anchored. 28

LIST OF FIGURES

Figure 1: The study area for Submerged Aquatic Vegetation (SAV) modeling in New Jersey and Long Island, New York, USA, 2015–2016, 256 random placed sample points to sample submerged aquatic vegetation (SAV, including 174 predicted SAV points and 82 null points). 8

Figure 2: The reaching capabilities of brant for eelgrass and floating biomass as modified from the original diagram from Clausen (2000). The letter *f* represents the floating biomass (added for this study), l_i represents individual leaf length, *r* for reaching capabilities of brant, and *x* the total water depth at mean low-low water (MLLW). 17

Figure 3: The NDVI range of -0.048 to -0.060 (in green) which was used for field efforts to identify potential SAV in the study area, shown here near Barnegat Light, New Jersey, November 2015 – February 2016. Also visible are the potential presence/absence points that were sampled in this area. 29

Figure 4: The eelgrass predicted presence for intertidal New Jersey established using an NDVI for initial field efforts. Followed by determining top field collected covariates to create a model average equation which included water depth, NH_3-N, and water temperature. The resulting presence/absence map was then divided after the optimal threshold was determined (threshold = 0.24).Figure 4*a* shows all eelgrass predicted and Figure 4*b* shows the eelgrass presence after limiting the raster area to 56 cm to reflect the brant reaching depth and average shoot length sampled. 30

Figure 5: The predicted presence for *Ulva* (Figure 5*a*) and Rhodophyta (Figure 5*b*) for New Jersey. The covariates used in the model average equation for *Ulva* included water depth, water temperature, NH_3-N, and turbidity. The covariates used in the model average equation for Rhodophyta were water depth, water temperature, NH_3-N, and salinity. The resulting presence/absence maps were then divided with a 0.26 threshold for *Ulva* and a 0.33 threshold for Rhodophyta. 31

Figure 6: The predicted presence of all studied SAV species for Long Island, New York. Figure 6*a* shows total eelgrass predicted presence (threshold = 0.24), Figure 6*b* shows the predicted eelgrass presence after limiting the raster area to 56 cm to reflect the brant reaching depth and average shoot length sampled. Figure 6*c* shows *Ulva* predicted presence (threshold = 0.26) and Figure 6*d* shows Rhodophyta predicted presence (threshold = 0.33). 32

ABSTRACT

Submerged aquatic vegetation (SAV), e.g. eelgrass (*Zostera marina*), and macroalgae (*Ulva lactuca., Enteromorpha spp., Gracilaria tikvahiae*) provides critical ecosystem functions. However, because of a changing coastal environment due to shifting climates and anthropogenic land alteration, it is becoming more important to protect this ecosystem. There is a need to create a predictive remotely sensed model to assess SAV abundance and thus potentially long-term degradation. Secondarily, because SAV has many benefits to organisms including the Atlantic brant (*Branta bernicula hrota*), which is a specialist on these food sources, building a predictive model will aid in assessing the potential energetic carrying capacity of wintering brant. To meet this need, I used Landsat 8 imagery to create a Normalized Difference Vegetation Index (NDVI) of potential SAV between the southern coast of Long Island, New York and intertidal zones of New Jersey, USA, December 2015-February 2016. To quantify the accuracy of this index, I assessed SAV presence at two hundred and fifty-six 900 m^2 sample sites including 174 predicted SAV points and 82 null points. Further at each site, I collected SAV biomass within a 1 m^2 quadrat, as well as two subsamples within the 900 m^2 resolution. A series of microhabitat variables were collected at each sample site to better evaluate predicted presence including water depth, water temperature, NH_3 – N, turbidity, bottom type, and salinity. The NDVI correctly identified presence of eelgrass with 46% accuracy and the *Ulva*/*Enteromorpha* and Rhodophyta with 61% accuracy. Using 22 a priori general linear models and AIC model averaging, *Ulva/Enteromorpha* was significantly

predicted by water depth and NH_3-N, Eelgrass was significantly predicted by NH_3-N, and Rhodophyta was best predicted by water depth. Using the top averaged models, I produced predictive maps that show the potential presence/absence of SAV species throughout the study area and extrapolated presence to available biomass. Estimates of energetic carrying capacity for both study areas were similar to mid-winter survey population counts for 2015–2016, thus further validating the accuracy of the NDVI predictive modeling.

Chapter 1

BUILDING A MODEL OF SUBMERGED AQUATIC VEGETATION FOR ATLANTIC BRANT

Introduction

There has been increasing concern regarding sea-level rise and natural disasters from severe storms which may negatively impact the resiliency of environmentally sensitive aquatic areas such as intertidal bays and coastal salt marshes (Burkett and Kusler 2000, Duarte et al. 2002, Kemp et al. 2004). While seagrass ecosystems only comprise about 0.1–0.2% of the global ocean area, they provide valuable ecosystem services such as stabilizing suspended sediments, improving water clarity, wave attenuation, and as habitat for aquatic and wildlife species (Duarte et al. 2002). Additionally, anthropogenic influences such as agricultural herbicide runoff, erosion of fine grain sediments, and nutrient enrichment with associated algal growth have further degraded saltmarsh and intertidal bay quality (Kemp et al. 1983). One indicator of coastal aquatic health is the presence and abundance of Submerged Aquatic Vegetation (SAV). Any change in abundance and distribution of SAV due to natural environmental stochasticity as well as anthropogenic degradation (e.g. commercial boating or dredging, development, and/or recreation boating and propeller scarring) could have direct implications for species that rely on this as a food source or protective habitat (Bergstrom et al. 2006, Shaughnessy 2011). Because saltmarsh habitats and SAV attract migrating and wintering waterfowl for food and protective cover, changes in habitat availability or quality could also significantly impact

waterfowl food availability, spatial distribution, and energetic carrying capacity (Ward et al. 2005, Nichols et al. 2011).

Important SAV species of interest in the Mid-Atlantic region of the United States includes eelgrass (*Zostera marina*), varieties of macroalgae such as *Ulva lactuca* and *Enteromorpha spp.*, and numerous Rhodophyta (red/brown algae) species including *Spyridia filamentosa* and *Gracilaria tikavhiae*. Eelgrass on the East Coast of North America has been found to grow in medium to high salinity (15–30 ppt) and typically have a more narrow, shorter leaf size than eelgrass found on the West Coast of North America (Bergstrom et al. 2006). Eelgrass performs many ecosystem functions including an essential food and habitat for crabs, scallops, and fish (Bergstrom et al. 2006). Eelgrass on the East Coast has been of special concern because of a population decrease from a slime mold wasting disease (*Labyrintha zosterae*) in the early 1930s dubbed "the most destructive mortality in the history of plant pathology" (Cottam and Munro 1954).

Ulva lactuca, commonly referred to as sea lettuce, grows in diverse salinity and can range in density based on available nutrient levels in the water (Bergstrom et al. 2006). It has been found to both stick to underwater medium as well as float freely (Bergstrom et al. 2006). This mobility can also make it more difficult to estimate *Ulva* densities available in an area. Additionally, sea lettuce can become a nuisance in high nutrient-rich water thus, smothering other SAV, negatively affecting commercial clamming, and harming other aquatic organisms that benefit from SAV (Bergstrom et al. 2006). *Enteromorpha* is a relative of the Ulvaceae family and is a fine, hair-like algae that can also grow in almost any salinity and is commonly found mixed in with or mistaken as pieces of *Ulva* (Bergstrom et al. 2006). The primary Rhodophyta

present in the Mid-Atlantic is graceful red weed (*Gracilaria tikvahiae*) which is free-forming or attached to structures and is highly competitive in a variety of nutrient, salinity, and water temperature values (Hill 2001). It is most commonly found in areas < 1 m of water, grows <30cm high, and present in a variety of colors ranging from darker green to a reddish/brown color, dependent on the habitat (Hill 2001).

The Atlantic brant *(Branta bernicula hrota*), hereafter brant, have been a species of interest because their population has consistently fluctuated from 1955 to present, raising the question of what is causing this instability (Heise et al. 2019, Ladin et al. 2011, Nissley et al. 2016, United States Fish and Wildlife 2019). Brant are unique among waterfowl in their exclusive use of the intertidal zone while wintering in the Mid-Atlantic region. Furthermore, brant are a specialist consumer of SAV in their winter distribution and thus SAV has a direct effect on brant distribution, survival, reproductive success, and population size (Cottam et al. 1941, Cottam and Munro 1954, Ward et al. 2005, Ladin et al. 2011, Shaughnessy 2011). Demonstrating their dependency on SAV, historic brant diet consisted of over 80% eelgrass. When a slime mold, *Labyrinthula sp.*, was introduced to the Atlantic Flyway in 1930, it decimated the existing eelgrass beds, which led to a decrease in eelgrass abundance and subsequently led to a stark decrease in brant population of 90–98% by 1934 (Cottam et al. 1941). Additionally, Cottam and Munro (1954) noted this decreased eelgrass abundance and population decrease altered brant principal wintering grounds; shifting north from Pamlico Sound, North Carolina to New Jersey and Long Island, New York. Dietary impacts are still seen today as wintering brant now feed on 53–55% macroalgae, 18% eelgrass, 17–22% salt marsh cordgrass (*Spartina alterniflora*), and 8–9% terrestrial grass (*Poaceae. sp.)* (Ladin et al. 2014). Although eelgrass is not

presently their primary food source (Ladin et al. 2011), it still has the potential to play a critical role for wintering brant on the Atlantic Flyway (as it still does on the Pacific Flyway) (Shaughnessy et al. 2012).

Because of this specialist relationship between SAV and brant, the Arctic Goose Joint Venture Strategic Plan prioritized the need for a "cost effective survey to index wintering habitats" (Arctic Goose Joint Venture Technical Committee 2008). Additionally, in 2012, Hurricane Sandy hit the New Jersey coastline becoming the largest Atlantic hurricane on record. Due to the environmental impact on intertidal bay areas, the integrity of SAV beds was questioned and the need to monitor them was heightened. In response, the United States Congress and the United States Fish and Wildlife Service funded a series of restoration and research projects to investigate coastal habitat resiliency including SAV presence predictions.

My research received funding by the United States Fish and Wildlife Service to create a cost-effective predictive model of SAV to use on post-Hurricane Sandy monitoring. Predictive models of SAV that rely on analyses of high resolution imagery (< 1 m x 1 m ground sample distances) allows for areas of seagrass and other habitats to be identified readily over large geographic domains on the order of 10^2 square kilometers (Lathrop et al. 2006). Although such high resolution imagery potentially provides an efficient method developing a detailed model of SAV presence, it is costly and time consuming to acquire the data and to ensure images are collected under suitable conditions (good sun angle, low tide, low wind, and low water turbidity, Lathrop et al. 2006). As a cost-effective and accessible alternative, lower resolution LANDSAT 8 images (i.e., 30 m x 30 m ground sample distance) are collected over the same locales every 16 days (United States Geological Survey 2017). These images are

publicly available and allow for the potential construction of an available and predictive SAV model. Because of the lower resolution of the Landsat data, the presence of photosynthetic vegetation relies on the commonly applied Normalized Difference Vegetation Index (NDVI) in which ratios of near-infrared and red bands in the images are used to identify areas of significant photosynthetic vegetation.(Weier and Herring 2000. Pettorelli et al. 2005, Cho et al. 2008).

In addition to remote sensing imagery for predicting SAV, there are numerous environmental variables that are known to affect SAV presence and growth including water temperature, salinity, light attenuation (turbidity and depth), coastal storms/sudden change in environment, water quality (nutrient loading), and human influence (Flynn and Chapra 2014, Patrick et al. 2014, Unsworth et al. 2015). With this knowledge and to assure accuracy in predictive power, field collected covariates are necessary to predict the presence of SAV.

I have four objectives with this research. First, the NDVI is calculated using Landsat 8 imagery to identify locales of SAV in the intertidal waters in New Jersey and Long Island, New York where wintering brant are most numerous. Second, a subsample of sites that are potentially high in SAV based on the NDVI calculations were visited during the winter of 2015–2016 to verify and quantify the presence/absence of SAV species. Third, while visiting these sites, additional data regarding water depth, water temperature, water turbidity, salinity, bottom type, and levels of NO_3-N and NH_3-N were collected to determine if they better predict SAV presence. Last, at each site, to subsample biomass of the three primary SAV species (eelgrass, *Ulva*, and Rhodophyta species) to determine the energetic food availability for brant. These data allow for the extrapolation of site energy to a landscape level

energetic carrying capacity. The outcome of this thesis research has the potential to aid Federal agencies with information for future intertidal resiliency-planning by offering a relatively simple and cost-effective method to predict SAV presence. This process will all be applicable for building carrying capacity models for Atlantic brant which can provide better conservation strategies.

Study Area

Atlantic brant wintering range occurs from North Carolina through the northeast region, United States, with the highest density (~90%) of Mid-Winter Surveyed birds occurring in coastal New Jersey and New York (Baldassare 2014, U.S. Fish and Wildlife Service 2016). These areas house a variety of submerged aquatic vegetation species determined from a prior preliminary field season as well as from Rutgers University and the United States Fish and Wildlife Service (Lathrop and Haag 2011, P. Castelli personal communication). Based on this, our primary study area for measuring and building a model of intertidal SAV was along the northern half of New Jersey and the south side of Long Island, New York (Figure 1). Sampling in intertidal waters of Long Island, New York ranged from Shirley, New York (40° 46' 55.79" N, -72° 42' 23.19" W) to Jamaica Bay, New York (40° 35' 29.02" N, 73° 50' 10.71" W), and samples in intertidal waters of New Jersey ranged from Silverton, New Jersey (40° 0' 33.83" N, 74° 5' 40.77" W) to Margate City, New Jersey (39° 20' 44.20" N, 74° 31' 53.82" W).

Figure 1: The study area for Submerged Aquatic Vegetation (SAV) modeling in New Jersey and Long Island, New York, USA, 2015–2016, 256 random placed sample points to sample submerged aquatic vegetation (SAV, including 174 predicted SAV points and 82 null points).

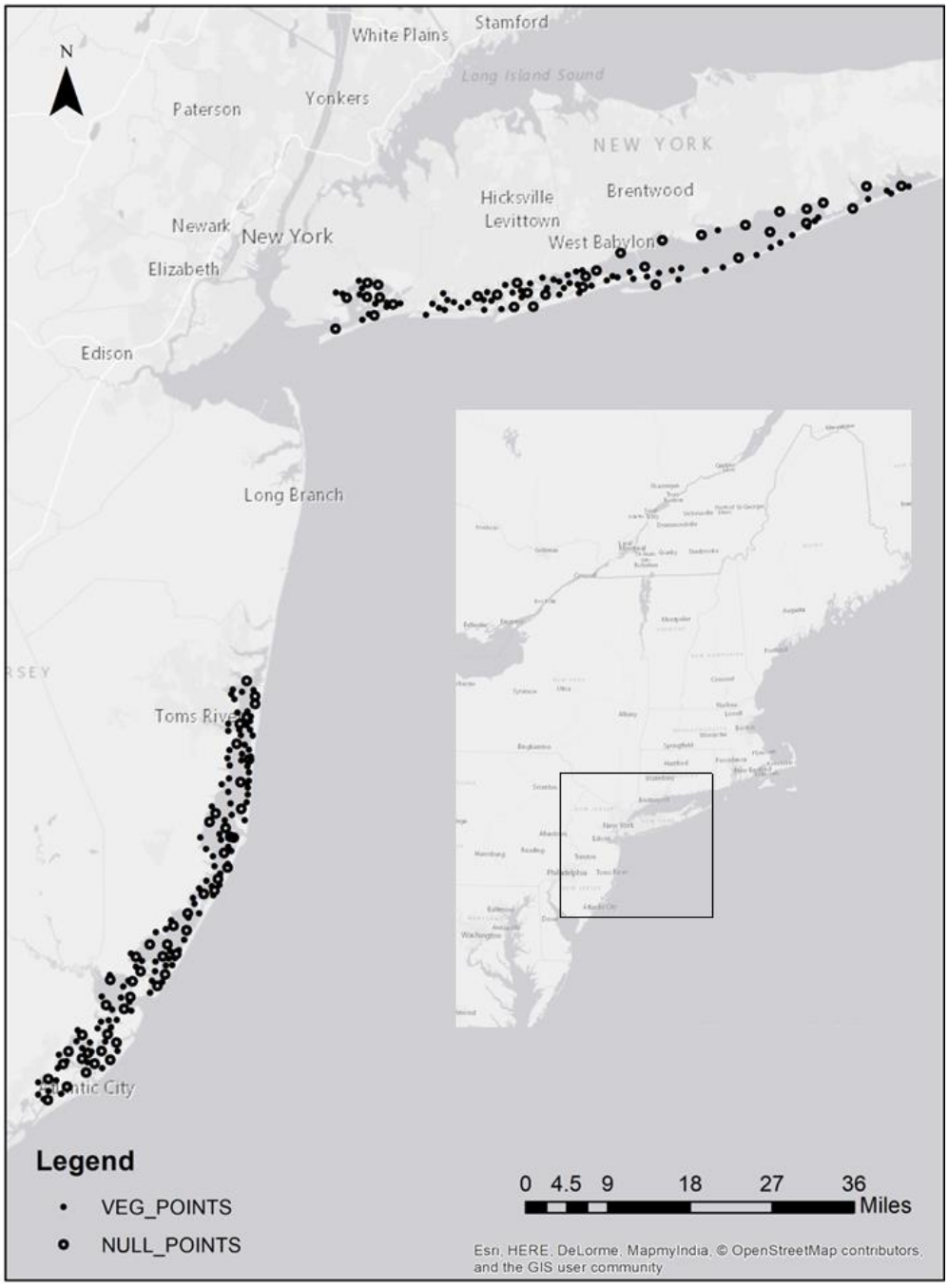

Methods

Initial mapping of potential submerged aquatic vegetation

The prediction of locales with submerged aquatic vegetation (SAV) within the study domain relies on implementation of the Normalized Difference Vegetation Index (NDVI) from using two of the spectral bands of data in LANDSAT 8 imagery. NDVI is ideal for this goal because green plants have low spectral reflectance in red and high reflectance in the near infrared that makes vegetation in an image easy to separate from other common land surface covers (Cho et al. 2008). Specifically, Chlorophyll *a* and *b* absorb energy in blue and red wavelengths for photosynthesis while the mesophyll absorb energy in the near-infrared region (NIR) (Cho et al. 2008). Thus, NDVI is calculated through the equation

$$NDVI=(NIR-Red)/(NIR+Red) \quad \text{Equation 1}$$

and delivers a range of values that reflects vegetation densities. Higher positive values are indicative of dense vegetation while a zero would suggest no vegetation (Weier and Herring 2000). Negative values suggest potential cloud cover, snowfall, or in the case of looking at water bodies, submerged vegetation (Weier and Herring 2000). Because of the 16 day repeat cycle for Landsat data collection, imagery used for this project were obtained for acquisition dates just prior to field validation and sampling efforts (i.e., between October and December 2015) to ensure the most up-to-date imagery was available to be compared with SAV field collection. All Landsat 8 images were processed using ENvironment for Visualization Images (ENVI) software; however, the calculation of NDVI is simple and can be completed in a variety of commercial and freely available applications that are readily obtainable. The NDVI data from ENVI were exported as geotiff's and imported into ArcGIS where they are

easily combined with other spatial data in an accurate geographic framework. Within ArcGIS, the NDVI range of -1 to 1 are easily classified with individual breaks to identify the range for SAV presence. These individual breaks were identified and synthesized from knowledge of historic eelgrass locations and a preliminary field effort to identify eelgrass location prior to implementing this methodology. This then allowed a created range that reflects the predicted SAV presence.

Field Collection of SAV and Environmental Covariates:

Field verification of the areas with significant SAV from the NDVI calculation was completed at 256 random points throughout the study site including 174 predicted vegetation points and 82 null points for validation of predicted SAV presence. Given the 30 m ground sample distance of LANDSAT imagery, each random sample area was 900 m^2. Therefore, each locale was surveyed and sampled as close to low tide as possible. For Long Island, sampling was completed between November and December 2015 and in New Jersey between December 2015 and February 2016. Sampling was conducted from an 1860 G3 VBW boat with a Garmin Echomap 54DV chartplotter with Garmin DownVü capabilities to have high-resolution sonar visualization when arriving at sample sites. In many locales, areas with dense grass beds were able to be viewed from using the DownVü prior to leaving the boat for sampling. Upon arrival at the site, if the site was > 2 m deep or on land, I removed the point from further analysis, and it was not sampled. If the depth was <2 m, I navigated directly to the point. Clausen (2000) estimated that brant can only reach down to roughly 0.4 m into the water to reach attached vegetation. However, I conservatively used 2 m depth to assure collection of SAV from sites where tidal fluctuation could potentially allow brant access to free floating SAV or tall stationary eelgrass at mean lower low water

(MLLW) level. Depending upon the area being sampled, most locations required ideal weather conditions (low wind and water movement) to ensure a proper sample collection and safety.

To estimate SAV biomass/m^2 for predicting energetic carrying capacity, I collected three subsamples of SAV within each 900 m^2 sample site, using a 1 m x 1 m x 2 m mesh covered quadrat (to prevent vegetation from moving out of the quadrat with water flow). I collected all SAV within the quadrat using a lake rake, which is made to cut through aquatic vegetation and allows optimal vegetation harvest. Collection within the quadrat consisted of many passes with the rake in several directions to ensure all rooted and floating vegetation was gathered. This was established through visibly inspecting the site and confirming no vegetation was remaining; or if the water was too turbid, until there was no vegetation remaining on the rake. Vegetation contained within the quadrat was collected and cleaned in between sample sites to make sure there was no cross-contaminating collection at sample sites. Floating biomass was collected when present using a 1 m net within a 10 m^2 area surrounding the sample site to ensure sufficient representation of the surrounding area; however, only a few sample sites had floating biomass present so this was not a significant factor in field collection data. Once an SAV sample, from both raking and potential floating biomass, it was deposited into a freezer-safe zipper plastic bag and frozen until field collection was finished.

At each sampling point, I also collected other data including metrics for water turbidity, water depth, water temperature, salinity, bottom type, and a water sample for future ammoniacal nitrogen (NH_3-N) and nitrate nitrogen (NO_3-N) level analysis. I collected salinity using a salinity refractometer and water turbidity using a 0.2 m

Secchi disk to determine water clarity (United States Environmental Protection Agency 2012). Water samples were collected in 118 ml containers and frozen. Lastly, bottom type (sand versus mud) was determined from raking the bottom or feeling the bottom type when walking the site. To ensure appropriate landscape-level extrapolation, NOAA MLLW LiDAR was used to represent our water depth metric.

Laboratory Analysis

In the laboratory, I thawed SAV samples and cleaned them thoroughly to remove all mud and debris. For each of the three subsamples per sampling point,I then sorted all SAV by species and if eelgrass was present, I measured the length of 10 random shoots per sample to estimate the average eelgrass length observed in the study area. This measurement was necessary to estimate available leaf biomass (A_i) using a modified equation from Clausen (2000, Figure 2):

$$A_i = \sum_{i=f}^{n} f + \sum_{i=l}^{n} l_i - (x - r) \; for \; x > r; \; l_i \geq (x - r) \qquad \text{Equation 2}$$

where f = total floating biomass, x = water depth at mean lower low water, r = brant reaching capability, and l_i = the length of individual eelgrass. While the total non-floating leaf biomass can be determined using the equation $T = \sum_{i=l}^{n} l_i$, the available leaf biomass must be corrected for water depth and reach length (Clausen 2000). This correction is utilized only when leaf length is greater than or equal to this difference between water depth and reach. It is predicted no vegetation will be available $A_i = 0$ when leaf length is less than the difference of the depth subtracted by the reach length ($l_i < [x - r]$). In contrast, the proportion of available leaf biomass will be available 100% for floating biomass if $x > r$.

With the available vegetation sorted, I placed the samples in an oven for 48 hours at 50^{o} C to ensure they are properly dried and then I measured their dry mass

(Ladin 2011). I estimated the available energy for brant by multiplying each species dry mass by its True Metabolizable Energy (TME) (*Ulva/Enteromorpha/*Rhodophyta = 14.552 kJ/g and eelgrass =14.627kJ/g) (Kirby and Obrecht 1980) and corrected by the proportion of the plant that was within the brant feeding range (per Equation 2, Clausen 2000). I then created a sampling point average from the three subsamples giving an average value per 1 m^2 and then extrapolated the average to our 900 m^2 sampling point size by multiplying this result by 900.

Analysis and modeling

To evaluate whether any microhabitat covariates could predict SAV presence, I conducted binomial logistic regression within a Generalized Linear Model (GLM) framework to predict the presence of each SAV species (eelgrass, *Ulva*, Rhodophyta) via seven covariates (water depth, water temperature, water turbidity, salinity, bottom type, NH_3-N and NO_3-N levels) via 22 a priori models. I first tested for correlation between variables and found NH_3-N was strongly correlated with NO_3-N. Therefore, I used NH_3-N lowering the number of tested variables to six. I then established the a priori models by determining combined covariates that would best predict SAV presence. I created 22 a priori models that ranged from singular covariates to a larger combination of covariates that could have a more significant result for predicting presence. All a priori models were compared using Akaike Information Criterion corrected for small sample size (AICc, Burnham and Anderson 2002). If ΔAIC value were ≤ 2, I conducted weighted model averaging to determine the beta values for the best predicted covariates. For model averaged parameter estimation, I used the "zero method" where a parameter estimate (and error) of zero is substituted into those models where the given parameter is absent thus reducing the effect sizes (and errors)

of predictors that only appear in models with small model weights (particularly when the predictors have weak effects) (Burnham and Anderson 2002, Grueber et al. 2011).

After covariate modeling to predict SAV presence, I created base maps for each covariate using Spline Interpolation in ArcGIS (ESRI 2016*a*). Spline interpolation estimates values using a function that minimizes overall surface curvature (Childs 2004). Due to my predictive variables being spatially gradual and continuous, spline interpolation of their values extrapolated to the landscape created a smooth surface that passed through all of my input points (Childs 2004). Once this was completed, these spline base maps were used in the "Raster Calculator" function of ArcGIS and I completed a spatial regression analysis by using model averaged beta values estimated for each of the SAV species (Regression Analysis Basics ESRI 2016*b*). With these spatial regression maps complete, SAV presence/absence maps were then put into the "Extract Values to Points" ArcGIS tool to extract the values of the sample points with presence/absence values. I formatted the presence values from the rasters created with their ground-truthed presence/absence and then input them into Program R to determine the optimal thresholds. Using the package "PresenceAbsence", I was able to determine the percent correctly classified (PCC), sensitivity, specificity, Kappa, and area under curve (AUC) for each threshold used (Freeman and Moisen 2008). Additionally, I used the package's MaxSens+Spec option which determined the threshold that maximizes the sum of sensitivity and specificity (Youden's index, Freeman and Moisen 2008). The goal of this method was to minimize both the mean error rates for positive and negative observations (sensitivity + specificity – 1) (Freeman and Moisen 2008); however, this method has also been noted to cause lower thresholds to a lower sample size which could then

overpredict the distribution of the area (Manel et al. 2002). I also compared my thresholds to the standard 0.50 threshold to ensure the MaxSens+Spec was displaying a more accurate representation of the data.

To estimate carrying capacity for brant, I estimated "Goose-Energy Days" (GED):

$$GED_{ATBR} = \frac{Landscape_E}{DEE_{ATBR}} \quad \text{Equation 3}$$

I used a brant daily energy expenditure (DEE) of 1,594.98 ± 85.57 kJ/day which Heise (2012) estimated from 24-hour behavioral scan samples from. To estimate landscape energy ($Landscape_E$), I averaged the species-specific abundances of the sampled vegetation types. For *Ulva* and Rhodophyta, I multiplied the average observed biomass/1 m^2 sampling unit by the known energy availability of 14.552 kJ/g (Ladin et al. 2011) and then extrapolated to the total ha of predicted presence. The resulting total energy was then divided by the DEE to get the total GED. To ensure an accurate carrying capacity, the total GED was divided by 180 days which is the estimated length of brant wintering. For eelgrass, it was first necessary to develop maps at each centimeter depth in "Raster Calculator" to determine the percentage of eelgrass available to brant based off their reaching depth (40 cm) combined with the average eelgrass shoot length making the assumption they can only clip off and consume what they can reach. I then converted the rasters to point values using ArcMap's "Raster to Point". I narrowed the values to only the threshold value of predicted presence, eliminating all of the pixels that did not display presence. I totaled and compared this number against each cm level to determine the variation of eelgrass availability and the amount of additional energy available at each centimeter change. A second theoretical model was created assuming brant could pull up and consume a full eelgrass shoot if it could reach the shoot. The estimated biomass per 1 m^2 from the two

models was multiplied by the known energy availability of 14.627 kJ/g (Ladin et al. 2011) and then extrapolated to the total ha of predicted presence.

Figure 2: The reaching capabilities of brant for eelgrass and floating biomass as modified from the original diagram from Clausen (2000). The letter *f* represents the floating biomass (added for this study), l_i represents individual leaf length, *r* for reaching capabilities of brant, and *x* the total water depth at mean low-low water (MLLW).

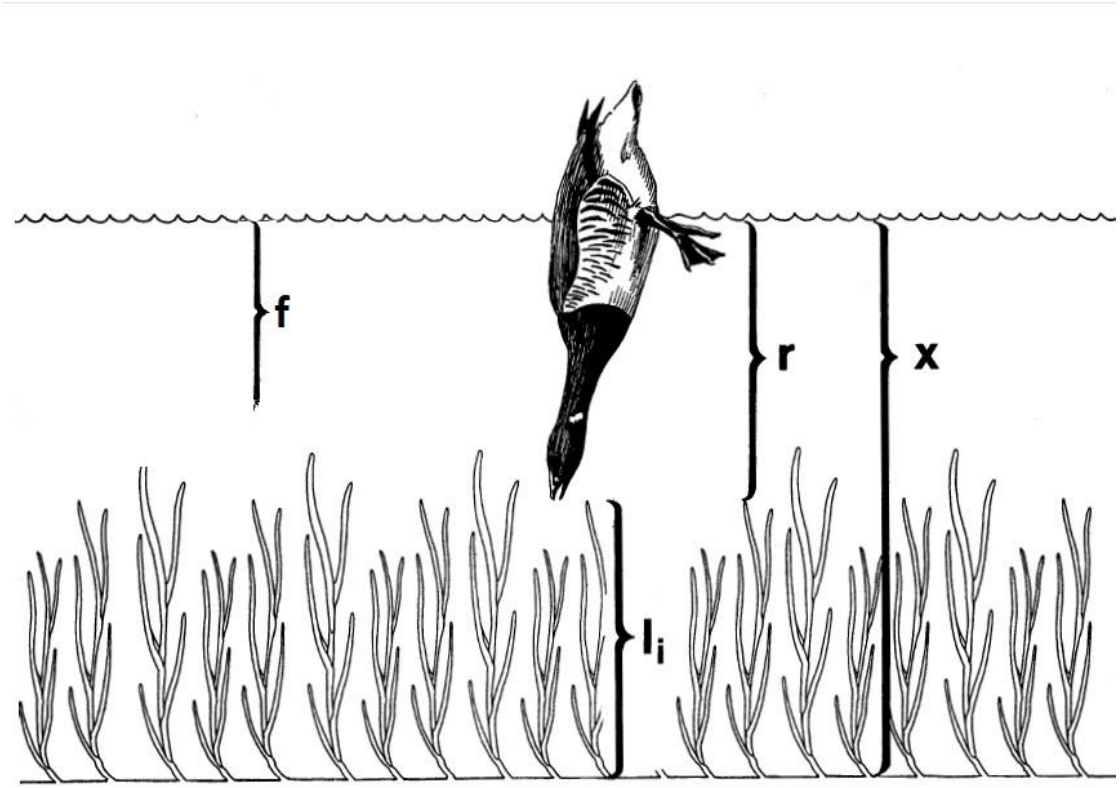

Results

Using the historic eelgrass bed knowledge, preliminary field efforts, and knowing an approximate range of SAV reflectance from previous NDVI studies, I was able to narrow down an NDVI range that could predict SAV presence. The results of the NDVI calculation are presented in Figure 3 where areas of SAV are present in the range of -0.048 to -0.060. I randomly chose 100 points (67 vegetation and 33 null points) in the New York study area, and 156 points (107 vegetation and 49 null points) in the New Jersey study area to validate SAV presence. The number of sample points was selected to keep an even distribution of points throughout both study areas to ensure accurate collection of data.

Using data from the field survey, I completed model validation to assess the accuracy of detecting each SAV species from NDVI predictions including the amount of error that occurred during field collection (Table 1). The largest observed errors occurred because of excessive water depth (n = 20), sandbar/SAV depletion (n = 11), followed by terrestrial grass/marsh (n = 7), false negatives (n = 5), and commercial clam beds (n = 2). The percentage accuracy of predicting eelgrass was 46%, *Ulva/Enteromorpha* was 61%, Rhodophyta was 61%, and total sites containing SAV was 71% (Table 2). It is important to note that of this accuracy, five null points (four in Long Island and one in New Jersey) contained SAV which were included in the overall accuracy assessment since it was a small percentage of points.

My second goal was to predict SAV presence from site specific environmental variables. This utilized all 256 original sample sites, although 50 were omitted during modeling due to missing covariate information. For each SAV species, I built 22 a priori models testing the effect of water depth, water temperature, salinity, bottom

type, and NH_3-N (Tables 3–5). Three models were plausible predictors of *Ulva*/*Enteromorpha* presence including 1) water depth + NH_3-N + turbidity (ΔAIC = 0, ω = 0.44), 2) water depth + water temp + turbidity + NH_3-N (ΔAIC = 1.36, ω = 0.223), and 3) water depth + NH_3-N (ΔAIC = 1.39, ω = 0.220) (Table 3). In all three models, the Wald Chi-square hypothesis test of parameter significance showed only water depth was significant ($P < 0.01$). The weighted model average equation for *Ulva*/*Enteromorpha spp.* presence = 0.902 [SE 0.473] + (1.366 [SE 0.344] × water depth) + (-0.010 [SE 0.0139] × water temp) + (-0.254 [SE 0.197] × NH_3N) + (0.621 [SE 0.378] × turbidity) (AICc combined weight = 0.74).

Two models were plausible predictors of eelgrass presence including 1) water depth + water temp + NH_3-N + turbidity (ΔAIC = 0.00, ω = 0.50), and 2) water depth + NH_3-N + turbidity (ΔAIC = 1.90, ω = 0.19) (Table 4). In both models, the Wald Chi-square hypothesis test showed water depth was significant ($P = 0.01$), however in the second model NH_3-N was also significant ($P = 0.04$). The weighted model average equation for eelgrass presence = -0.146 [SE 0.473] + (0.609 [SE 0.230] × water depth) + (0.064 [SE 0.033] × water temp) + (-0.343 [SE 0.033] × NH_3-N) + (0.539 [SE 0.389] × turbidity) (AICc combined weight = 0.75).

For Rhodophyta algae, four models were plausible predictors including 1) water depth + salinity + NH_3-N (ΔAIC = 0.00, ω = 0.32), 2) water depth + NH_3-N + turbidity (ΔAIC = 0.49, ω = 0.25), 3) water depth + NH_3-N (ΔAIC = 0.60, ω = 0.23), 4) water depth + water temp + NH_3-N + turbidity (ΔAIC = 1.90, ω = 0.12) (Table 4). Across all the models, the Wald Chi-square hypothesis test showed only water depth was significant ($P < 0.01$). The weighted model average equation for Rhodophyta presence = -0.203 [SE 0.906] + (1.540 [SE 0.347] × water depth) + (-0.005 [SE 0.007]

× water temp) + (0.202 [SE 0.192] × NH_3-N) + (0.034 [SE 0.021] × salinity) (AICc combined weight = 0.80).

Using the top averaged models, I produced predictive maps that showed the potential presence/absence of SAV species throughout the study area. The optimal threshold was determined in R using the MaxSens+Spec option and was compared to a standard 0.5 threshold to show the higher percent correctly classified, sensitivity, and specificity of the MaxSens+Spec (Table 6).The maps were then adjusted with the appropriate threshold value (Figures 5-6). For eelgrass, the threshold was 0.24 with 91% correctly classified as actual eelgrass locations, but only 54% of sites classified as without eelgrass. *Ulva* had a threshold of 0.26 with 90% correctly classified as *Ulva* presence locations, but only 60% of sites were correctly classified as without *Ulva*. Rhodophyta had a threshold of 0.33 with 88% correctly classified values with Rhodophyta presence locations, but only 63% were correctly classified as without Rhodophyta (Table 6). Lastly, Figure 4*b* and 6*b* show the example of the limited availability due to depth limitation for brant feeding and the assumption that they can only clip a portion of the eelgrass.

The estimated carrying capacity for brant across the study area was as followed: *Ulva* was estimated to support 50,071 $\pm$ SE 6,515 brant and Rhodophyta was estimated to support 94,600 $\pm$ SE 5,253 brant (Table 7). For eelgrass, it was necessary to correct available biomass by the availability of eelgrass shoot length. The average eelgrass shoot length was 15.57cm that I rounded to 16 cm (SE ±0.39) to simplify use with corresponding depth values in my spatial mapping. Thus, using the average 16 cm shoot length and 40 cm reaching length, I considered 56 cm the maximum reaching depth for brant to clip or pull up eelgrass. If a brant could reach an

eelgrass shoot and pull up the entire plant for consumption, I estimated eelgrass would support 38,845 $\pm$ 2,772 total brant across the study area (Table 7). However, if I make the assumption that brant clip the available eelgrass shoot without pulling up the entire plant, I predicted eelgrass would support 20,741 ± 3,746 brant over the study area. Thus, the total brant supported from all SAV would be 183,516 ± 14540 if brant pulled up the entire shoot of eelgrass and 165,412 ± 15514 if brant were clipping eelgrass at centimeter depth increments beyond 40 cm.

Table 1: The sampling errors that occurred when conducting field collection of SAV in New Jersey and Long Island, New York, USA, 2015-2016.

Sampling Errors			
Type of Error	New Jersey	Long Island	Total
Deep water	15	5	20
Terrestrial grass/marsh	0	7	7
Sandbar/depletion	5	6	11
Commercial clam bed	2	0	2
False negative (SAV on null)	1	4	5
Total	27	25	52

Table 2: Of the total number of sites that NDVI predicted SAV (eelgrass, *Ulva/Enteromorpha*, and Rhodophyta) present (New Jersey [n=107] and Long Island, New York [n=67], USA, 2015-2016, the number and percent accuracy of study sites that SAV was physically observed. This includes the five (4 from Long Island and 1 from New Jersey) null samples that included SAV.

	N presence (% accuracy)		
Vegetation Type	New Jersey	Long Island	Total
Eelgrass	45/107 (42%)	35/67 (52%)	80/174 (46%)
Ulva/Enteromorpha	64/107 (60%)	42/67 (63%)	106/174 (61%)
Rhodophyta	63/107 (59%)	43/67 (64%)	106/174 (61%)
Total sites with SAV	71/107 (66%)	53/67 (79%)	124/174 (71%)

Table 3: Twenty-two a priori models (AICc, ΔAIC, and AIC weight ω values) predicting the presence of *Ulva* and *Enteromorpha* from 6 site level environmental variables in intertidal New Jersey and Long Island, New York, 2015–2016.

Model	k	AICc	Δ AIC	$\boldsymbol{\omega}$
Water depth + NH_3 + turbidity	4	225.83	0	0.44
Water depth + water temp + NH_3 + turbidity	5	227.19	-1.36	0.22
NH_3 + water depth	3	227.21	-1.39	0.22
Water depth + salinity + NH_3	4	229.15	-3.32	0.08
Full	7	231.06	-5.24	0.03
NH_3 + turbidity	3	257.42	-31.60	0
Water temp + NH_3 + turbidity	4	258.82	-32.99	0
Water depth	2	263.52	-37.69	0
Water depth + salinity	3	263.99	-38.16	0
Water depth + water temp	3	264.01	-38.18	0
Water depth + water temp + salinity	4	265.01	-39.19	0
Water depth + bottom type	3	265.13	-39.3	0
Water depth + water temp + bottom type	4	265.88	-40.06	0
Water depth + water temp + salinity + bottom type	5	266.88	-41.06	0
NH_3	2	274.74	-48.91	0
NH_3 + salinity	3	274.89	-49.07	0
Turbidity	2	291.74	-65.92	0
Null	1	316.04	-90.21	0
Water temp	2	316.86	-91.03	0
Bottom type	2	317.51	-91.68	0
Salinity	2	317.77	-91.94	0
Water temp + salinity	3	318.36	-92.54	0

Table 4: Twenty-two a priori models (AICc, ΔAIC, and AIC weight ω values) predicting the presence of eelgrass from 6 site level environmental variables in intertidal New Jersey and Long Island, New York, 2015–2016.

Model	k	AICc	Δ AIC	$\boldsymbol{\omega}$
Water depth + water temp + NH_3 + turbidity	5	223.81	0.00	0.50
Water depth + NH_3 + turbidity	4	225.71	-1.90	0.19
NH_3 + water depth	3	225.93	-2.11	0.17
Full	7	227.80	-3.99	0.07
Water depth + salinity + NH_3	4	227.86	-4.05	0.07
Water temp + NH_3 + turbidity	4	237.63	-13.82	0
NH_3 + turbidity	3	240.27	-16.45	0
NH_3	2	248.24	-24.43	0
NH_3 + salinity	3	249.60	-25.79	0
Water depth + water temp + salinity	4	261.80	-37.99	0
Water depth + water temp	3	261.86	-38.05	0
Water depth	2	262.46	-38.65	0
Water depth + salinity	3	263.28	-39.46	0
Water depth + water temp + salinity + bottom type	5	263.61	-39.79	0
Water depth, water temp, and bottom type	4	263.72	-39.91	0
Water depth and bottom type	3	263.95	-40.14	0
Turbidity	2	277.29	-53.48	0
Water temp	2	288.31	-64.49	0
Bottom type	2	288.92	-65.11	0
Null	1	289.34	-65.53	0
Water temp and salinity	3	290.19	-66.38	0
Salinity	2	291.33	-67.52	0

Table 5: Twenty-two a priori models (AICc, ΔAIC, and AIC weight ω values) predicting the presence of *Rhodophyta* algae from 6 site level environmental variables in intertidal New Jersey and Long Island, New York, 2015–2016.

Model	k	AICc	Δ AIC	$\boldsymbol{\omega}$
Water depth + salinity + NH_3	4	226.83	0.00	0.32
Water depth + NH_3 + turbidity	4	227.32	-0.49	0.25
NH_3 + water depth	3	227.43	-0.60	0.23
Water depth + water temp + NH_3 + turbidity	5	228.74	-1.90	0.12
Full	7	229.56	-2.72	0.08
Water depth	2	266.78	-39.94	0
Water depth + water temp	3	267.14	-40.31	0
NH_3 + turbidity	3	267.26	-40.43	0
Water depth + bottom type	3	268.25	-41.42	0
Water temp + NH_3 + turbidity	4	268.76	-41.93	0
Water depth + salinity	3	268.77	-41.94	0
Water depth + water temp + bottom type	4	268.94	-42.11	0
Water depth + water temp + salinity	4	269.01	-42.18	0
Water depth + water temp + salinity + bottom type	5	270.81	-43.98	0
NH_3 + salinity	3	278.57	-51.74	0
NH_3	2	283.41	-56.57	0
Turbidity	2	304.05	-77.22	0
Water temp + salinity	3	326.81	-99.98	0
Salinity	2	326.94	-100.11	0
Null	1	327.99	-101.16	0
Water temp	2	328.70	-101.87	0
Bottom type	2	329.42	-102.59	0

Table 6: The calculated optimal thresholds determined in R to show the presence/absence thresholds for each SAV species from New Jersey and Long Island, New York, USA, 2015-2016. The optimal thresholds were then compared to an arbitrary threshold of 0.5.

	Threshold	PCC	Sensitivity	Specificity	Kappa	AUC
Ulva	0.5	0.685	0.346	0.832	0.193	0.76
	0.26	0.693	0.897	0.603	0.408	0.76
Eelgrass	0.5	0.704	0.063	0.917	-0.026	0.73
	0.24	0.630	0.906	0.539	0.311	0.73
Rhodophyta	0.5	0.708	0.488	0.819	0.319	0.76
	0.33	0.716	0.884	0.632	0.447	0.76

Table 7: The estimated carrying capacity for *Ulva/Enteromorpha*, Rhodophyta, and eelgrass assumptions of a complete pull of eelgrass and an assumption that clipping of eelgrass occurs in centimeter increments after their 40 cm reaching capability for Long Island, New York and coastal New Jersey, USA during winter 2015-2016. The estimated carrying capacity for both algae types assuming they are not depth limited due to the ability to be free floating and not permanently anchored.

	Ulva		Rhodophyta		Eelgrass (<56 cm) Pull		Eelgrass (<56 cm) Clip	
	New Jersey	Long Island	New Jersey	Long Island	New Jersey	Long Island	New Jersey	Long Island
Predicted area present (ha)	15,864.93	14,257.53	13,999.23	14,513.67	8,723.7	11,476.26	8,723.7	11,476.26
Biomass (g/m^2) when present	3.28 ± 0.60		6.55 ± 0.71		3.77 ± 0.47		3.77 ± 0.47	
Total (± SE) biomass on landscape (kg) (in thousands)	520.28 ± 95.42	467.57 ± 85.75	916.35 ± 99.90	950.03 ± 103.57	329.27 ± 41.09	433.17 ± 54.06	201.52 ± 41.09	205.58 ± 54.06
True metabolizable energy (kJ/g)	14.55		14.55		14.63		14.63	
Total (± SE) available energy (kJ) (in billions)	7.57 ± 1.39	6.80 ± 1.25	13.34 ± 1.45	13.83 ± 1.51	4.82 ± 0.60	6.34 ± 0.79	2.95 ± 0.60	3.01 ± 0.79
Total (± SE) Goose Energy Days (in millions) assuming brant DEE = 1594.98 ± 85.57kj/day	4.75 ± 0.62	4.27 ± 0.56	8.36 ± 0.46	8.67 ± 0.48	3.02 ± 0.22	3.97 ± 0.28	1.85 ± 0.28	1.89 ± 0.39
Energetic Carrying Capacity (180 days)	26,371 ± 3,431	23,700 + 3,084	46,447 ± 2,579	48,154± 2,674	16,776 ± 1,197	22,069 ± 1,575	10,267 ± 1,547	10,474 ± 2,199
			94,600 ± 5,253					
Total energetic carrying capacity across both study areas	50,071 ± 6,515				38,845 ± 2,772		20,741 ± 3,746	

Figure 3: The NDVI range of -0.048 to -0.060 (in green) which was used for field efforts to identify potential SAV in the study area, shown here near Barnegat Light, New Jersey, November 2015 – February 2016. Also visible are the potential presence/absence points that were sampled in this area.

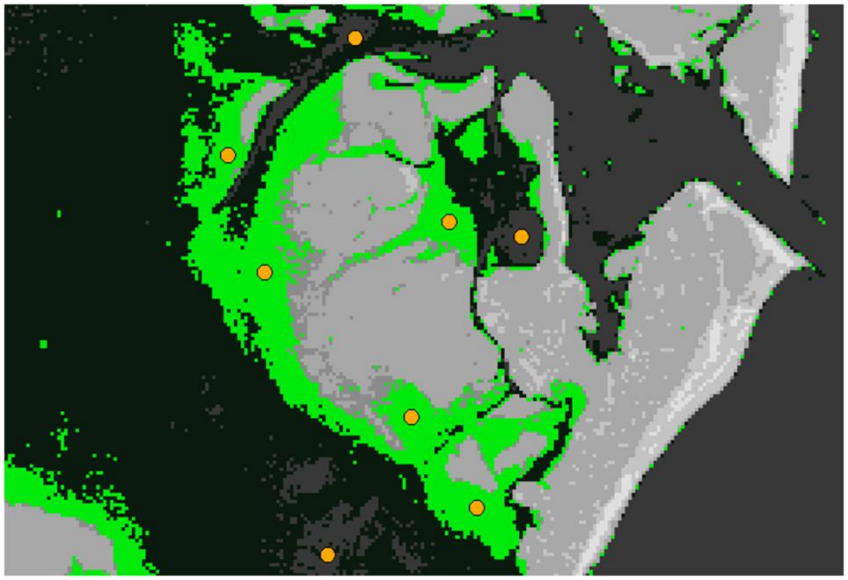

Figure 4: The eelgrass predicted presence for intertidal New Jersey established using an NDVI for initial field efforts. Followed by determining top field collected covariates to create a model average equation which included water depth, NH_3-N, and water temperature. The resulting presence/absence map was then divided after the optimal threshold was determined (threshold = 0.24).Figure 4*a* shows all eelgrass predicted and Figure 4*b* shows the eelgrass presence after limiting the raster area to 56 cm to reflect the brant reaching depth and average shoot length sampled.

Figure 4*a*

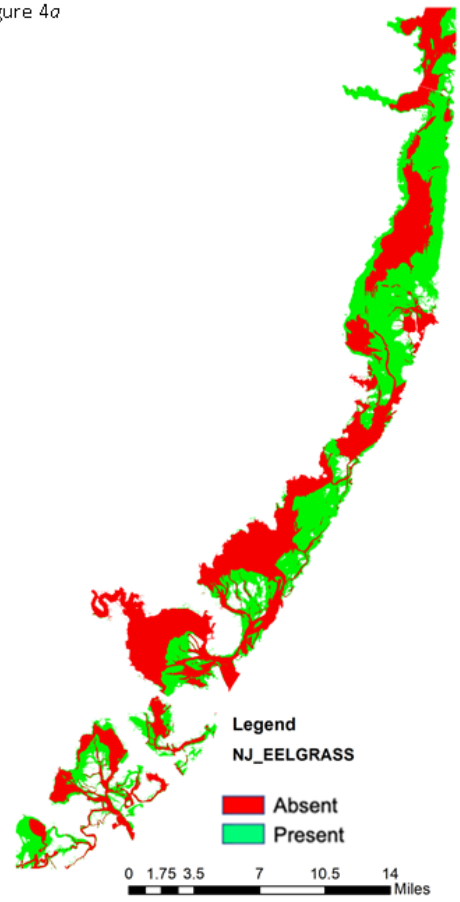

Figure 4*b*

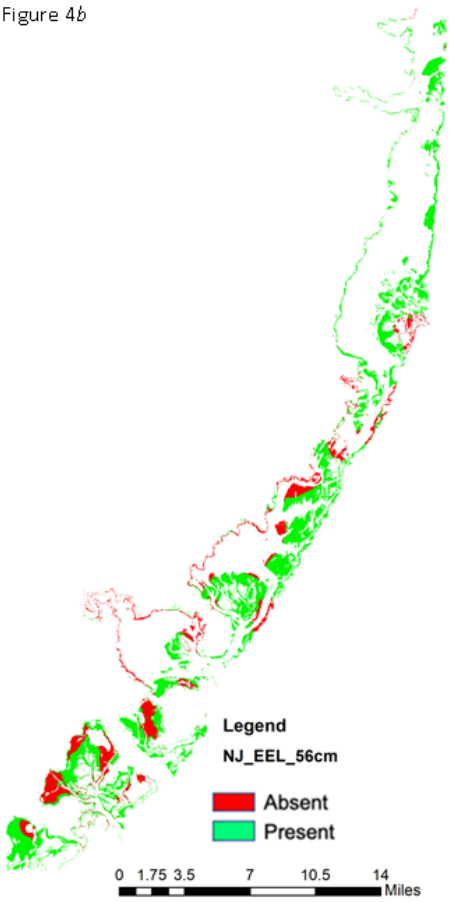

Figure 5: The predicted presence for *Ulva* (Figure 5*a*) and Rhodophyta (Figure 5*b*) for New Jersey. The covariates used in the model average equation for *Ulva* included water depth, water temperature, NH_3-N, and turbidity. The covariates used in the model average equation for Rhodophyta were water depth, water temperature, NH_3-N, and salinity. The resulting presence/absence maps were then divided with a 0.26 threshold for *Ulva* and a 0.33 threshold for Rhodophyta.

Figure 5*a*

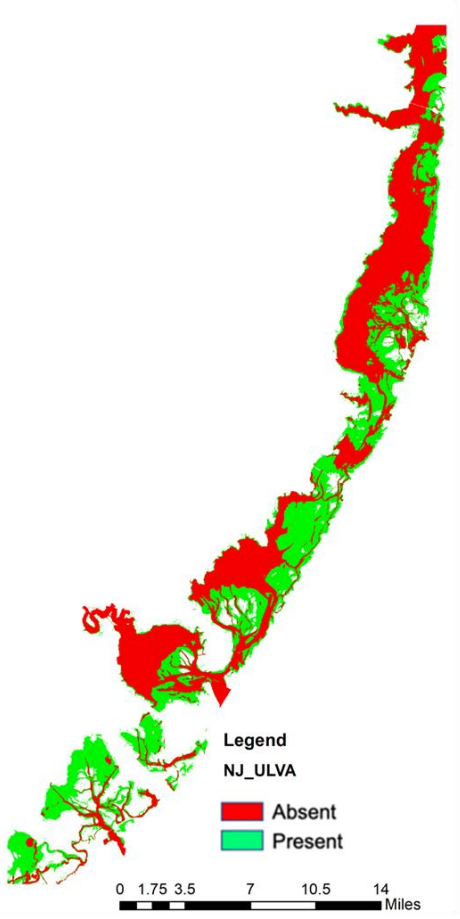

Figure 5*b*

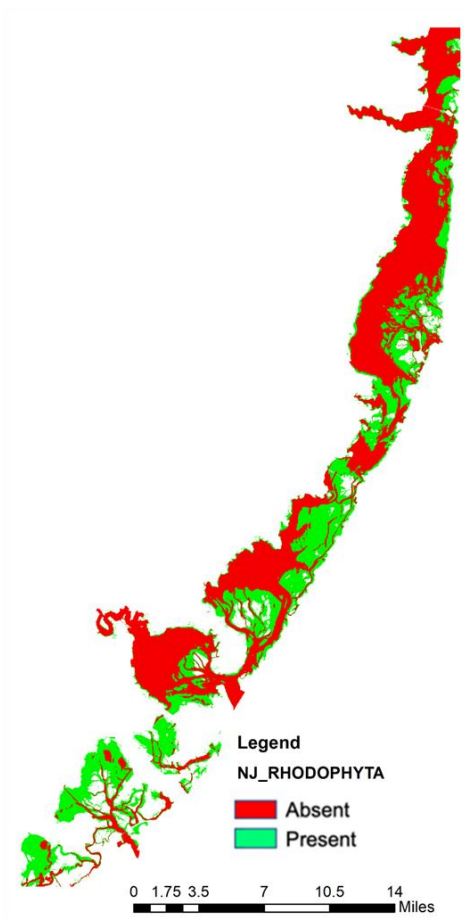

Figure 6: The predicted presence of all studied SAV species for Long Island, New York. Figure 6*a* shows total eelgrass predicted presence (threshold = 0.24), Figure 6*b* shows the predicted eelgrass presence after limiting the raster area to 56 cm to reflect the brant reaching depth and average shoot length sampled. Figure 6*c* shows *Ulva* predicted presence (threshold = 0.26) and Figure 6*d* shows Rhodophyta predicted presence (threshold = 0.33).

Figure 6*a*

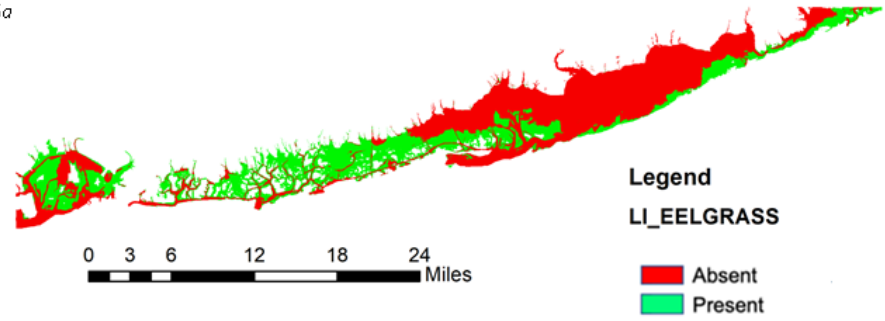

Figure 6*b*

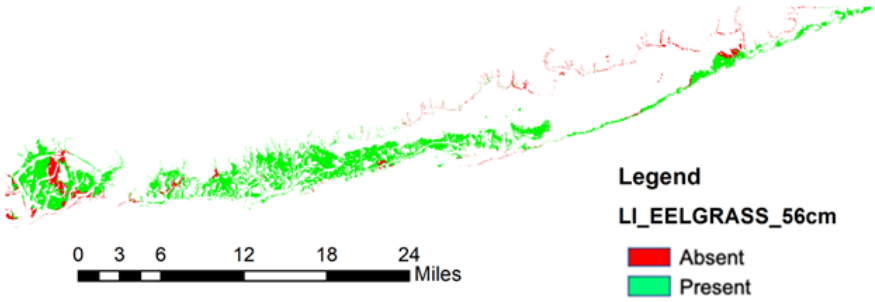

Figure 6*c*

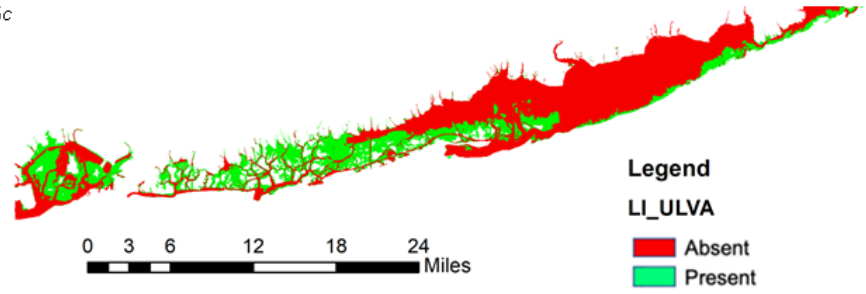

Figure 6*d*

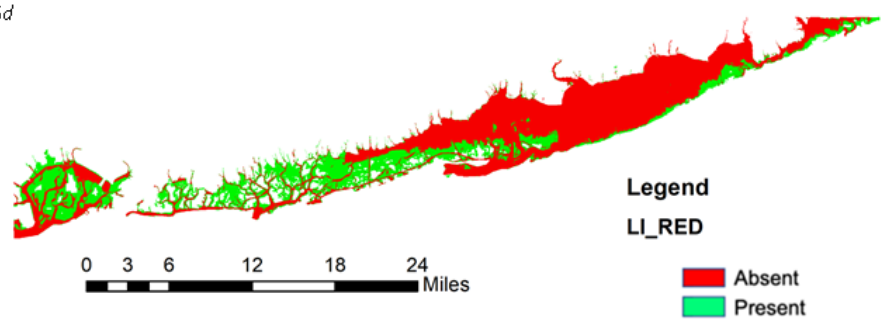

Discussion

The importance of having a predictive model for SAV is relevant for many organizations. With only 0.1–0.2% of the global ocean area consisting of seagrass ecosystems, it is crucial to have accurate and relevant knowledge of existing grass beds to better understand how to manage them. The goal of this research was to create a cost-effective model of submerged aquatic vegetation for coastal resiliency evaluation with the implication for estimating Atlantic brant energetic carrying capacity. By utilizing Landsat imagery and a Normalized Difference Vegetation Index, I was able to create a model that predicted SAV presence with an accuracy of 71% throughout all sample sites. Species specific accuracy was 46% for eelgrass and 61% for Rhodophyta and *Ulva*. These percentages were established from determining all sample sites that contained a biomass value for each species collected. Although species coverage can vary substantially throughout a large landscape such as my study areas, these numbers suggest a potential higher accuracy than previous studies (Beget and Di Bella 2007, Cho 2008). Other research using NDVI for submerged aquatic vegetation had accuracy issues due to the alteration of spectral response data when water levels vary (Beget and Di Bella 2007, Cho 2008). As water depth increases, spectral response can become less accurate and can increase the margin of error in predicting SAV.

Although NDVI-based range was able to properly locate SAV to a reasonable extent; there are many potential sources for both Type II errors (false negatives) and Type I errors (false positives). First, I identified five points with Type II error that NDVI did not predict as SAV, but were verified with in-situ sampling to show dense

vegetation. All five points were within the Long Island study area, but there were no Type II errors in the New Jersey study area. These five points were slightly outside of the predicted pixel range and thus I could have adjusted the NDVI range; however, it would have risked overestimating the vegetation and increasing Type I errors elsewhere in the study area. Second, there were multiple points that showed Type I errors. I was able to identify three potential sources of this error. First, some sites (N=20) were found to be in water > 1.22 m (4 ft) that were determined to be too deep for brant to feed. With some of the samples in channelized areas, it was difficult to determine true SAV presence. Excessive depth limited our sampling if SAV was present on the seafloor or if there had been algae present, whether anchored or floating, when the image was taken. Rooted SAV such as eelgrass cannot survive in excessively deep water due to the lack of light attenuation, increased competition with macroalgae, and turbidity (Choice et al. 2014). Accuracy of NDVI with increasing depth was found to be quickly diminishing in other studies, so it is not surprising that some of our deeper sites had no SAV or an error in predicting presence (Cho 2008).

The second source of Type I error was associated with sample sites that were terrestrial plants, mudflats, or sandbars. Although the NDVI accurately identified green pigment for the terrestrial grass (n=7), it incorrectly identified the correct vegetation within the original NDVI range. All the sample sites were within the Long Island sampling area and were found on high marsh areas consisting of *Spartina alterniflora* or *Spartina patens* except for one which was located on a dock surrounded by trees. There were 11 sites that were either on sandbars or mudflats. Two sites in Long Island had remanence of eelgrass roots suggesting the grass bed could have been depleted or destroyed prior to sampling. There were also a few mudflat sample sites

that were not safe to sample due to their locations and lack of structure; however, macroalgae was suspected to be present. Lastly, 2 sample points in New Jersey were unable to be reached due to being inside of a commercial clamming area and not safe to reach to sample. This was also suspected to have some presence of macroalgae based on the samples collected near it; however, I was unable to confirm this. These points were removed from analysis due to lacking covariate information and sampling. Since the aforementioned points were unable to be reached safely to confirm presence, they were assumed to be errors in the NDVI due to their lack of bottom structure and inability to retain SAV for long periods of time.

A third source of Type I error experienced from the NDVI was the original set of Landsat imagery downloaded for Long Island revealed a lot of cloud errors, that were observed prior to sampling of these sites, thus another date of imagery had to be utilized while in-situ sampling was occurring, this dataset was more recent than the prior imagery and contained less cloud obstructions. When looking at all of the errors incurred, the NDVI correctly classified many of these samples as containing green pigment, whether that be potential algae on a mudflat or *Spartina* on marsh; however, it was, unfortunately, not submerged vegetation as predicted.

Despite the number of observed Type I and II errors, the building of this NDVI model has shown that it is possible to locate multiple SAV species with adequate accuracy using Landsat imagery. However, I acknowledge that because of the identified Type I and II errors, I recommend further site and temporal model validation to confirm the NDVI range is accurate for predicting SAV. For example, the time period for SAV collection and model validation was not during peak SAV growth but focused on the prime Atlantic brant consumption period. Thus, if the focus

of SAV identification is focused on coastal resiliency, I would recommend sampling occur in late spring through August in the Mid-Atlantic region (Bergstrom et al. 2006).

Because of the resolution of Landsat imagery, the accuracy of my SAV abundance may be biased; the primary sample point was supplemented with two replicated points in random directions at a distance of 30 m. Therefore, data may not lie completely within the proposed 900 m^2 area and may reflect the abundance of vegetation on directly adjacent portions of the images. However, the spatial accuracy of Landsat imagery has a ca. 10 m position accuracy and the sampling distance is well within the combined range. Although the additional samples from each locale provided averages of the SAV present, it was my observation that the density of rooted grass beds were significantly different so that the average of three points may have increased variance in abundance at some locales. Therefore, future biologists may wish to increase abundance sample size or explore higher resolution remotely sensed data with a smaller pixel size (assuming budget and time permits) to refine a more accurate estimate. This area is the result of using Landsat, whereas a higher resolution image would have much smaller pixel spacing and, thus, provide a more accurate sample area

In addition to NDVI predictions, AIC modeling of microscale habitat characteristics further helped to predict SAV presence. I identified the most important covariate for all three SAV species categories was water depth, which has been recognized as a key factor to successful SAV density and growth due to light attenuation. Light attenuation is directly affected by factors such as suspended sediment that will lead to increased turbidity, as well as increase of water nutrients

which increases macroalgae response thus, increasing turbidity (Queen and Graine 2006, Bostrom et al. 2014, Choice et al. 2014).

The second covariate found in all three species top models was NH_3-N that suggests water nutrients can be important in determining the growth of SAV (Duarte 1995, Pedersen and Borum 1997, Nixon et. al 2001), especially Ammonical nitrogen (Pedersen and Borum 1997, Aguiar et al. 2003). High nitrogen content commonly leads to lack of oxygen in water and also excessive algae growth, which potentially inhibits seagrass growth (Harlin and Thorne-Miller 1981, O'Neill et al. 2015). The higher abundance of algae could also be attributed to more runoff and development on the mainland side of the bay system. One of our highest density sites of *Ulva* was adjacent to a landfill that may have had excess nitrogen runoff as is typically found near wastewater treatment facilities and agricultural/industrial runoff (Nixon et al 2001, United States Geological Survey 2017). Further, I found that after sampling was completed in January of 2016, there were a higher percentage of samples that had algae than grasses. This could have occurred due to the excessive nitrogen levels promoting algae and reducing light from reaching seagrass beneath it, effectively killing it (Duarte 1995, Bostrom et. al 2014, Choice et al 2014).

The third common covariate in two of the three species models was turbidity. This covariate is another driver in water clarity and light attenuation, thus, it is an important factor in determining SAV presence (Queen and Graine 2006, Cho 2008). Turbidity and water depth can be correlated because higher turbidity can lead to a lack of light attenuation through water, similar to how a greater depth can be limiting to SAV growth (Duarte 1991, Queen and Graine 2006). Many of the grass beds that were found were on the barrier island side of the bay were typically less turbid with sandy

bottoms while the mainland side of the bay had higher abundance of algae with muddy bottoms and increased turbidity.

After AIC modeling was completed, I determined thresholds for all of the SAV species to improve overall accuracy of the SAV presence and absence predictive maps. Having a higher accuracy for presence/absence also allowed for better accuracy for estimating energetic carrying capacity for brant. I identified the MaxSens+Spec option to best suit my data because it allowed me to minimize the mean error rates for positive and negative observation (sensitivity + specificity – 1). Manel et al. (2002) and Freeman and Moisen (2008) warned this method could potentially over predict areas when there is not a very large sample size distribution throughout the study area. While it is possible this source of error contributed to some Type I error observed, the percentage correct classified was consistent for each species and the sensitivity (true positive rate) was high. However, the specificity (true negative rate) of the thresholds all seemed relatively low in comparison to the 0.50 threshold suggesting that there were less correctly classified true negatives and contributed to overestimation of actual presence.

As a final validation of my models, I compared predicted energetic carrying capacity estimates to the 2015–2016 Mid-Winter Waterfowl Survey (MWS) population counts of brant. If brant could pull up eelgrass and consume entire shoots (in addition to full consumption of *Ulva* and Rhodophyta), I estimated 89,595 $\pm$ 7,208 brant in New Jersey and 93,923 $\pm$ 7,333 in Long Island. If brant could only clip eelgrass, I estimated New Jersey would support 83,085 $\pm$ 7,558 brant and Long Island could support 82,327 $\pm$ 7,956 brant. The MWS predicted that New Jersey had 83,894 brant and Long Island had 57,265 thus showing tremendous parity between data sets.

While the results suggest more of an overestimation in Long Island, this could be due to lack of survey data in parts of Long Island, which was noted by the Arctic Goose Joint Venture suggesting that ground surveys might be more accurate in some areas of Long Island that cannot easily be flown over (Arctic Goose Joint Venture Technical Committee 2008). The other possibility for overestimation is related to the sensitivity and specificity of each species. As previously discussed, the MaxSens+Spec option utilized to establish the optimal thresholds had a high sensitivity, but lower specificity. Taking this into account, it is very possible that the amount of SAV availability according to my thresholds is overestimated due to a lower number of true negatives.

Despite the apparent similarity in datasets, I acknowledge a series of potential sources of bias hat may influence the predictability in brant energetic carrying capacity. First, Rhodophyta was the most prevalent SAV species and had the highest potential to support the brant energetic carrying capacity (94,600). However, while Ladin (2010) and Ladin et al. (2014) noted the majority of the wintering brant diet in Long Island New Jersey was macroalgae (from both gross foregut and stable isotope analysis), they did not discern between red and green algaes. Thus it is unknown if brant diet preference will readily consume the large amounts of red algae I found. If they do no not, my energetic carrying capacity will be overestimated. A second potential source of overestimation is the recognition that brant would not be the only species utilizing the SAV present while wintering and my models do not include depletion. Therefore, it would be a reasonable assumption that simply extrapolating the full SAV presence across 180 days may overestimate energetic availability. Further SAV is eaten by a myriad of dabbling and diving ducks that winter in the Mid-Atlantic region, and thus competition for food resources could reduce brant carrying

capacity (Munro and Perry 1983). Unfortunately, without estimating the SAV use of all species throughout the study area, it is difficult to calculate the rate of SAV depletion. Despite these potential overestimates, I acknowledge one large underestimate. Ladin et al. (2014) also found that grass/clover and saltmarsh cordgrass (8–9% and 19–23% respectively) can occur in the brant diet. However, because these upland species are not an output of the NDVI methodology and predictive modeling, I acknowledge that my carrying capacity estimates could be underestimated by roughly 30%, however, overall, my estimations could still be high due to my higher sensitivity and lower specificity.

The importance of having a predictive model for SAV is relevant for many organizations. With only 0.1–0.2% of the global ocean area consisting of seagrass ecosystems, it is crucial to have accurate and relevant knowledge of existing grass beds to best understand how to manage them. My model demonstrated that accurate predictive results were possible, as well as estimates of Atlantic brant carrying capacity. A goal for my research was to create a cost-effective and simplistic model for biologists to utilize for quantifying existing SAV, observing yearly changes in SAV beds, and be able to make more accurate management decisions for waterfowl based on the health and resiliency of these aquatic ecosystems. I achieved this through utilizing Landsat and NDVI which allowed me to create a framework for others to utilize in predicting SAV presence/absence using their existing knowledge of SAV location for their study area.

REFERENCES

Aguiar, A. B., J. A. Morgan, M. Teichberg, S. Fox, I., Valiela. 2003. Isotopic evidence of the relative effects of ambient and internal nutrient supply on the growth of *Ulva lactuca*. Biology 205:250–251.

Arctic Goose Joint Venture Technical Committee. 2008. Arctic Goose Joint Venture strategic plan: 2008–2012. Unpublished report, Arctic Goose Joint Venture Coordination Office, Canadian Wildlife Service, Edmonton, Alberta, Canada.

Baldassarre, G. A. 2014. Ducks, geese, and swans of North America. Johns Hopkins University Press, Baltimore, Maryland, USA.

Beget, M. and C., Di Bella. 2007. Flooding: The effect of water depth on the spectral response of grass canopies. Journal of Hydrology 335:285–294.

Bergstrom, P. W., R. F. Murphy, M. D. Naylor, R. C. Davis, and J. T. Reel. 2006. Underwater grasses in Chesapeake Bay and Mid-Atlantic coast waters: A guide to identifying submerged aquatic vegetation. Maryland Sea Grant College, College Park, Maryland, USA.

Boström, C., S. Baden, A. C. Bockelmann, K. Dromph, S. Fredriksen, C. Gustafsson, D. Krause-Jensen, T. Möller, S. Nielsen, B. Olesen, J. Olsen, L. Pihl, and E. Rinde. 2014. Distribution, structure and function of Nordic eelgrass (*Zostera marina*) ecosystems: Implications for coastal management and conservation. Aquatic Conservation Marine and Freshwater Ecosystems:410-434.

Burkett, V., and J. Kusler. 2000. Climate change: Potential impacts and interactions in wetlands of the United States. Journal of the American Water Resources Association 36:313–320.

Burnham, K.P., and D. R. Anderson. 2003. Model selection and multimodel inference: A practical information-theoretic approach. Springer Science & Business Media, New York, New York, USA.

Childs, C. 2004. Interpolating surfaces in ArcGIS Spatial Analyst. ArcUser July-September. ESRI Education Services.

Cho, H, P. Kirui, H. Natarajan. 2008. Test of multi-spectral vegetation index for floating and canopy-forming submerged vegetation. International Journal of Environmental Research and Public Health 5:477-483.

Choice, Z., J. Frazer, C. Jacoby. 2014. Light requirements of seagrasses determined from historical records of light attenuation along the coast of peninsular Florida. Marine Pollution Bulletin 8:94–102.

Clausen, P. 2000. Modelling water level influence on habitat choice and food availability for *Zostera* feeding brent geese *Branta bernicla* in non-tidal areas. Wildlife Biology 6:75–87.

Cottam, C., J. J. Lynch, and A. L. Nelson. 1944. Food habits and management of American sea brant. The Journal of Wildlife Management 8:36–56.

Cottam, C., and D. A. Munro. 1954. Eelgrass status and environmental relations. The Journal of Wildlife Management 18:449–460.

Duarte, C. M. 1991. Seagrass depth limits. Aquatic Botany 40:363–377.

Duarte, C. M. 1995. Submerged aquatic vegetation in relation to different nutrient regimes. Ophelia 41:87–112.

Duarte, C.M. 2002. The future of seagrass meadows. Environmental Conservation 29:192–206.

ESRI. 2016. How spline works. http://desktop.arcgis.com/en/arcmap/10.3/tools/spatial-analyst-toolbox/how-spline-works.htm. Last accessed 25 April 2020.

ESRI. 2016. Regression analysis basics. http://desktop.arcgis.com/en/arcmap/10.3/tools/spatial-statistics-toolbox/regression-analysis-basics.htm. Last Accessed 25 April 2020.

Grueber, C. E., S. Nakagawa, R.J. Laws, and I.G. Jamieson. 2011. Multimodel inference in ecology and evolution: challenges and solutions. Journal of Evolutionary Biology 24:699–711.

Flynn, K. F., and S. P. Chapra. 2014. Remote sensing of submerged aquatic vegetation in a shallow non-turbid river using an unmanned aerial vehicle. Remote Sensing 2014:12815–12836.

Freeman, E. A., and G. Moisen. 2008. PresenceAbsence: An R package for presence absence analysis. Journal of Statistical Software 23:1–31.

Harlin, M. M., and B. Throne-Miller. 1981. Nutrient enrichment of seagrass beds in a Rhode Island coastal lagoon. Marine Biology 65:221–229.

Heise, J. 2012. Incorporating nocturnal activity of wintering Atlantic brant (*Branta bernicla hrota*) into 24 hour time-activity and daily energy expenditure models. M.S. in Wildlife Ecology, University of Delaware, Newark, USA.

Heise, J., C.K. Williams, P.M. Castelli. 2019. Factors influencing a 24-hour time-budget for wintering Atlantic brant. Journal of Fish and Wildlife Management 10:79-90.

Hill, K. 2001. Indian River Lagoon Species Inventory. Smithsonian Marine Station at Fort Pierce. https://naturalhistory2.si.edu/smsfp/irlspec/Gracil_tikvah.htm. Last accessed 25 April 2020.

Kemp, W. M., W. Boynton, J. Adolf, D. Boesch, W. Boicourt, G. Brush, J. Cornwell, T. Fisher, P. Glibert, J. Hagy III, L. W. Harding, E. Houde, D. Kimmel, W. D. Miller, R. Newell, M. Roman, E. M. Smith, and J. Stevenson. 2005. Eutrophication of Chesapeake Bay: Historical trends and ecological interactions. Marine Ecology Progress Series 303:1–29.

Kemp, W. M., R. R. Twilley, J. C. Stevenson, W. R. Boynton, and J. C. Means. 1983. The decline of submerged vascular plants in upper Chesapeake Bay: Summary of results concerning possible causes. Marine Technology Society Journal 17: 78–89.

Kirby, R. E. and H.H. Obrecht. 1980. Atlantic Brant - human commensalism on eelgrass beds in New Jersey. Wildfowl 31:158–160.

Ladin, Z. S. 2010. Bioenergetic and food use of wintering and staging Atlantic brant. M.S. Thesis, University of Delaware, Newark, USA.

Ladin, Z. S., P. M. Castelli, S. R. McWilliams, and C. K. Williams. 2011. Time energy budgets and food use of Atlantic brant across their wintering range. Journal of Wildlife Management 75:273–282.

Ladin, Z. S., C. K. Williams, P. M. Castelli, K. Winiarski, J. Osenkowski, and S. R. McWilliams. 2014. Regional and intraseasonal variation in diet of wintering and staging Atlantic brant. Journal of Wildlife Management 7:1206–1215.

Lathrop, R. G., and S. M. Haag. 2011. Assessment of seagrass status in the Barnegat Bay - Little Egg Harbor estuary system: 2003 and 2009. Center for Remote Sensing and Spatial Analysis/ Institute of Marine and Coastal Sciences, School of Environmental and Biological Sciences, Rutgers University, New Jersey, USA.

Lathrop, R. G., P. Montesano, and S. Haag. 2006. A multi-scale segmentation approach to mapping seagrass habitats using airborne digital camera imagery. Photogrammetric Engineering and Remote Sensing 72:665–675.

Manel, S., H. Williams, and S. Ormerod. 2002. Evaluating presence-absence models in ecology: The need to account for prevalence. Journal of Applied Ecology 38:921–931.

Munro, R., and M. Perry. Distribution and abundance of waterfowl and submerged aquatic vegetation in Chesapeake Bay. 1983. United States Environmental Protection Agency. Chesapeake Bay Program Annapolis, Maryland., USA.

Nichols, J. D., M. D. Koneff, P. J. Heglund, M. G. Knutson, M. E. Seamans, J. E. Lyons, J. M. Morton, M. T. Jones, G. S. Boomer, and B. K. Williams. 2011.

Climate change, uncertainty, and natural resource management. The Journal of Wildlife Management 75:6–18.

Nissley, C. 2016. Assessing the impact of snow geese and cackling geese competition on breeding Atlantic brant on Southampton Island, Canada. M.S. Thesis, University of Delaware, Newark, USA.

Nixon, S., Buckley, B., Granger, S., Bintz, J. 2001. Responses of very shallow marine ecosystems to nutrient enrichment. Human and Ecological Risk Assessment 7: 1457–1481.

O'Neill, K., M. Schreider, L. McArthur, S. Schreider. 2015. Changed in the water quality characteristics during a macroalgal bloom in a coastal lagoon. Ocean and Coastal Management 118:32–36.

Patrick, C. J., D. E. Weller, X. Li, and M. Ryder. 2014. Effects of shoreline alteration and other stressors on submerged aquatic vegetation in subestuaries of Chesapeake Bay and the mid-Atlantic coastal bays. Estuaries and Coasts 37: 1516–1531.

Pedersen, M. F., and J. Borum. 1997. Nutrient control of estuarine macroalgae: growth strategy and the balance between nitrogen requirements and uptake. Marine Ecology Progress Series 161:155–163.

Pettorelli, N., J. O. Vik, A. Mysterud, J. M. Gaillard, C. J. Tucker, N. C. Stenseth. 2005. Using the satellite-derived NDVI to assess ecological responses to environmental change. Trends in Ecology and Evolution 20:503–510.

Queen, R., and J. Graine. 2006. SAV restoration handbook: A guide for restoring SAV on DOD installations. United States Army Environmental Center and Department of Defense Legacy Resource Management Program. Washington, D.C., USA.

Shaughnessy, F. J., W. Gilkerson, J. M. Black, D. H. Ward, and M. Petrie. 2012. Predicted eelgrass response to sea level rise and its availability to foraging black brant in Pacific coast estuaries. Ecological Applications 22:1743–1761.

United States Environmental Protection Agency. 2012. Using a secchi disk or transparency tube. Water: Monitor and assessment. http://water.epa.gov/type/rsl/monitoring/155.cfm. Last accessed 25 April 2020

United States Fish and Wildlife Service. 2016. Mid-winter waterfowl survey. United States Department of the Interior, Washington D.C., USA.

United States Fish and Wildlife Service. 2019. Waterfowl population status, 2019. United States Department of the Interior, Washington D.C., USA.

United States Geological Survey. 2017. Landsat Acquisition Tool. United States Department of the Interior, Washington D.C., USA. https://landsat.usgs.gov/landsat_acq. Last accessed 25 April 2020.

United States Geological Survey. 2017. Nitrogen and water. United States Department of the Interior, Washington D.C., USA. https://www.usgs.gov/special-topic/water-science-school/science/nitrogen-and-water?qt-science_center_objects=0#qt-science_center_objects. Last accessed 25 April 2020.

Unsworth, R. K. F., C. J. Collier, M. Waycott, L. J. Mckenzie, L. C. Cullen-Unsworth. 2015. A framework for the resilience of seagrass ecosystems. Marine Pollution Bulletin 100:34–46.

Ward, D. H., A. Reed, J. S. Sedinger, J. M. Black, D. V. Derksen, and P. M. Castelli. 2005. North American brant: Effects of changes in habitat and climate on population dynamics. Global Change Biology 11:869–880.

Weier, J., and D. Herring. 2000. Measuring vegetation (NDVI & EVI). NASA Earth Observatory. https://earthobservatory.nasa.gov/features/MeasuringVegetation. Last accessed 25 April 2020.